Vol. 30: 61–69, 2005 | CLIMATE RESEARCH Clim Res | Published December 19

Spatial patterns of the urban heat island in Zaragoza (Spain)

Sergio M. Vicente-Serrano[1,2,*], José M. Cuadrat-Prats[1], Miguel A. Saz-Sánchez[1]

[1]Instituto Pirenaico de Ecología, CSIC (Spanish Research Council), Campus de Aula Dei, PO Box 202, 50080 Zaragoza, Spain
[2]Unit for Landscape Modelling, University of Cambridge, Sir William Harding Building, Tennis Court Road, Cambridge CB2 1QB, UK
[3]Departamento de Geografía, Universidad de Zaragoza, Calle Pedro Cerbuna, Ciudad Universitaria, 50009 Zaragoza, Spain

ABSTRACT: Spatial patterns of the urban heat island (UHI) in Zaragoza (Spain) were determined by Principal Component Analysis (VARIMAX rotation) of air temperature in the city, and mapped using GIS. The 3 components extracted accounted for 92.9% of the total variance. Principal component (PC) 1 accounted for the most general patterns of UHI, PC2 showed a shift of warm areas to the SE and PC3 a shift to the NW. A rotated component matrix was used to identify correlations between each component and daily maps. The spatial patterns indicated by PC2 and PC3 were determined by surface wind direction. The displacement of warm areas to the SE (PC2) was greater during NW winds while the shift to the NW (PC3) was produced mainly by SE winds.

KEY WORDS: Urban climate · Urban heat island · Spatial patterns · Principal component analysis · Surface wind · Zaragoza · Spain

1. INTRODUCTION

Urbanization has led to substantial changes in land use, vegetation cover and other environmental parameters, and to the introduction of new elements and materials that can alter local surface–atmosphere energetic fluxes, thus disturbing regional climatic patterns.

One of the main effects of these alterations is increased inner city temperatures and the development of urban heat islands (UHIs), a general characteristic of medium- and large-scale urban environments (Arnfield 2003). These alterations present several common characteristics (reviewed by Landsberg 1981, Oke 1983, 1990, Atkinson 1985, Arnfield 2003). UHIs are characterized by positive temperature differences between a city and its outskirts, depending on the size and population of the city (Yamashita et al. 1986, Hogan & Ferrick 1988), which reach a maximum difference 3 to 5 h after nightfall (Oke & Maxwell 1975, Tereschenko & Filonov 2000).

The shape and intensity of UHIs are determined by geographical, structural and meteorological factors. For example, city park areas are relatively cold compared with built-up areas (Oke 1995, Dimoudi & Nikolopoulou 2003). Relief configuration (Beral-Guyonnet 1997) and urban geometry (Eliason 1994) also contribute to the shape and intensity of a UHI.

Nevertheless, the shape and intensity of UHIs are not stable, and their spatial and temporal variability may be significant. Improved knowledge of this variability is essential for urban management, bioclimatic comfort analysis and evaluation of atmospheric contaminant dispersion. Moreover, the spatial variability of a UHI is usually related to meteorological parameters such as wind direction (Kidder & Essenwanger 1995, Oke 1995, Magee et al. 1999, Morris et al. 2001). Gedzelman et al. (2003) studied the UHI of New York City and they stress that surface wind flows delay and reduce the intensity of the UHI and displace it about 10 km from its mean position. Also Szegedi & Kircsi (2003) show in Debrecen (Hungary) that the shape of UHI is usually altered by prevailing winds.

This study analyses the UHI of Zaragoza, one of Spain's largest urban areas. The objectives were to determine whether UHI patterns: (1) show important spatial differences and (2) are affected by local surface

*Email: svicen@ipe.csic.es

wind direction. For these purposes we used urban transects, surface interpolation techniques and multivariate statistics of a Geographical Information System (GIS).

2. STUDY AREA

The city of Zaragoza is located in NE Spain (Fig. 1) in the centre of the Ebro Valley (0° 52′ W, 41° 38′ N). It is the main industrial and commercial city of this region and occupies a plain of 159 km^2; in 2002 the city had a population of 620 000. It has a Mediterranean climate with a strong continental influence. The mean annual rainfall is just over 320 mm, with a maximum in May (38 mm) and minimum in August (21 mm). The mean annual temperature is 14.6°C, with cool winters (January: 6.2°C) and warm summers (July: 24.3°C). Winds are an important feature of the climate in the Ebro Valley. Two surrounding mountain ranges (the Pyrenees and the Iberian Range) isolate the valley from northerly and southerly flows, and winds are channeled in the valley in 4 dominant directions: WNW, NW, ESE, E. Westerly flows (W, WNW, NW, NNW) occur on 52% of the days, whereas ESE and E winds occur on 21% of the days.

The UHI in Zaragoza has been studied by Cuadrat (1993), Cuadrat et al. (1993), De la Riva et al. (1997) and Saz et al. (2003). The absolute maximum difference in the temperature between the city and the outskirts is about 6°C, with a mean UHI intensity of 2.5 to 3.5°C. The UHI of Zaragoza shows a negative gradient from the city center to the outskirts, which is consistent with the findings of studies in other cities. Nevertheless, on many days the warm areas of Zaragoza present a marked shift to the NW or SE areas of the city.

3. DATA AND METHODS

3.1. Spatial variability of the UHI

3.1.1. Data and quality control

UHIs can be analyzed using urban–rural differences in the data from weather stations or groups of weather stations (i.e. Adeabayo 1987, Philandras et al. 1999); networks of fixed stations within and around the city (i.e. Kuttler et al. 1996, Morris et al. 2001); or, mainly, transects across an urban area (i.e. Moreno 1994, Saaroni et al. 2000, Unger et al. 2001).

To determine the shape and temporal variability of the UHI in Zaragoza, we measured air temperature using digital thermometers mounted on 3 automobiles, at a height of 2 m above the ground. The thermometers had an accuracy of 0.1°C and the data were stored in the memory of the thermometers. The vehicles maintained a constant speed of 30 to 40 km h^{-1}. The data were taken

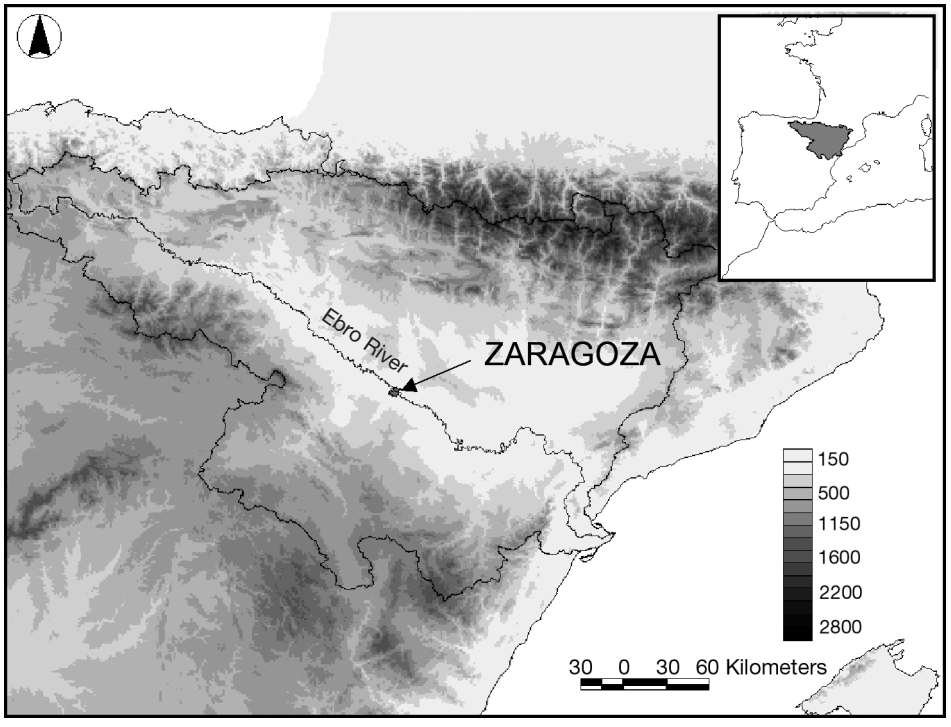

Fig. 1. Location of Ebro Valley and the city of Zaragoza

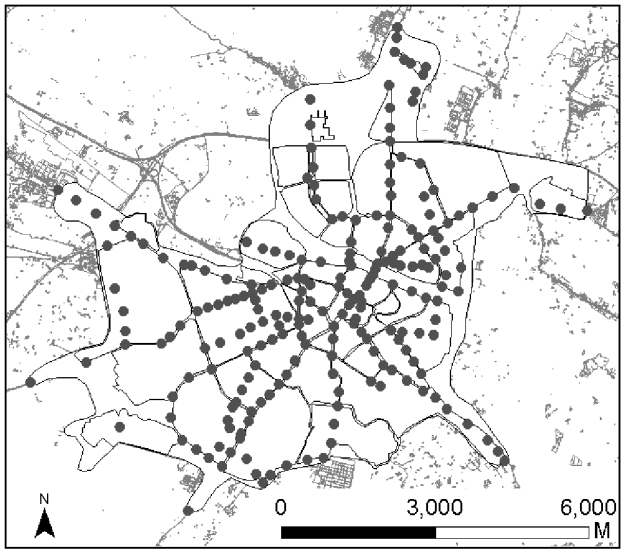

Fig. 2. Location of temperature measurements in Zaragoza

along 3 transects, which required about 1 h to absolve, and their totals length was 105 km. To represent the diversity of land use and building densities, data were compiled from 238 observation points distributed homogeneously within the city (Fig. 2). Data collection began 3 h after nightfall, because UHI intensity is greatest at this time (Tereshchenko & Filonov 2001). The measurement days were chosen randomly from July 2001 to September 2002. The final database contains the thermal data of 27 d at the 238 observation points.

Preliminary analysis showed a negative time trend related to nightly cooling, which must be eliminated to avoid a false spatial distribution of temperature (Winkler et al. 1981). The temperatures measured were therefore detrended and calculated for the same hour (central hour of the measurements) using lineal adjustments and residual values. Fig. 3 shows 2 examples of the correction procedure. The general pattern during the 27 d measured showed a linear decrease in temperature during nightly cooling. There were no non-linear relationships.

To guarantee temporal comparison among days, we standardized the daily data according to mean and SD. We used the Kolmogorov-Smirnoff test to determine the adjustment of thermal data to a normal distribution. On 20 d the data were considered normal (74.1% of daily samples). In cases of non-normality, natural logarithms were applied before standardization in order to fit the normal distribution more closely. This procedure does not affect the homogeneity of the data set. Thus, the magnitude of the standardised values obtained from the original temperatures and the log-transformation are spatially comparable.

This study aimed to determine the spatial patterns of air temperature. As the original thermal values on different days are not comparable, because absolute values and magnitudes differ, we analyzed the spatial patterns of UHIs from standardized daily temperatures. The main shortcoming of this procedure is that the magnitude of the UHI on each day is lost and cannot be used to analyze UHI intensity.

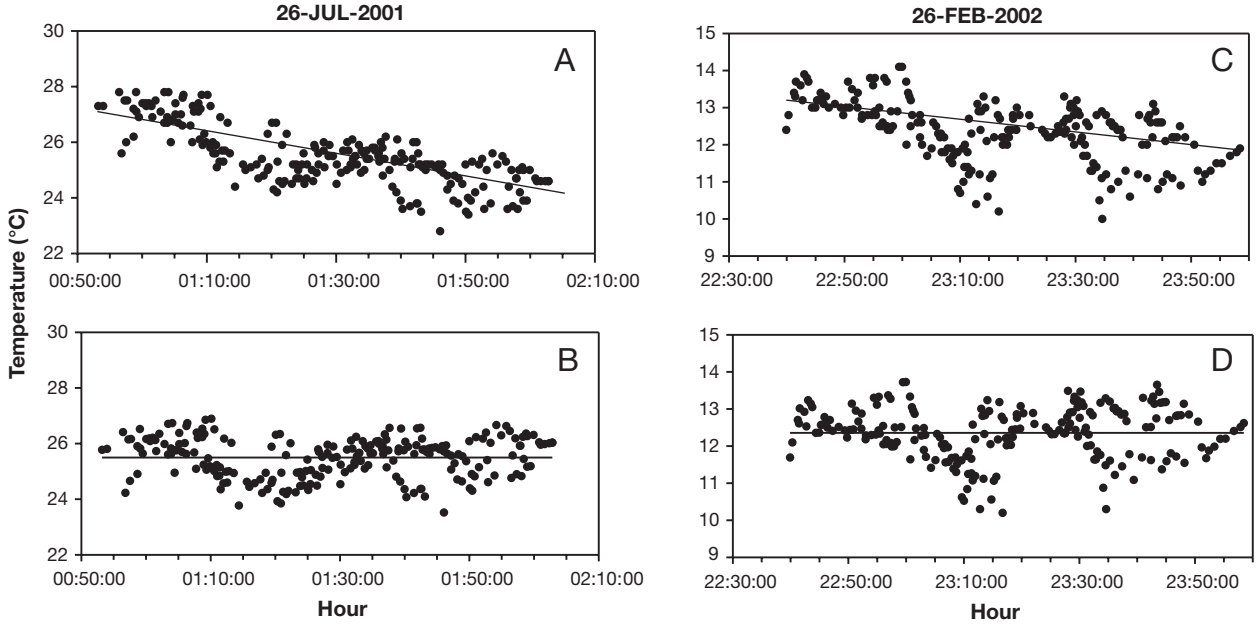

Fig. 3. Examples of the procedure to remove the effect of night cooling in temperatures; (A,C) original data, (B,D) detrended

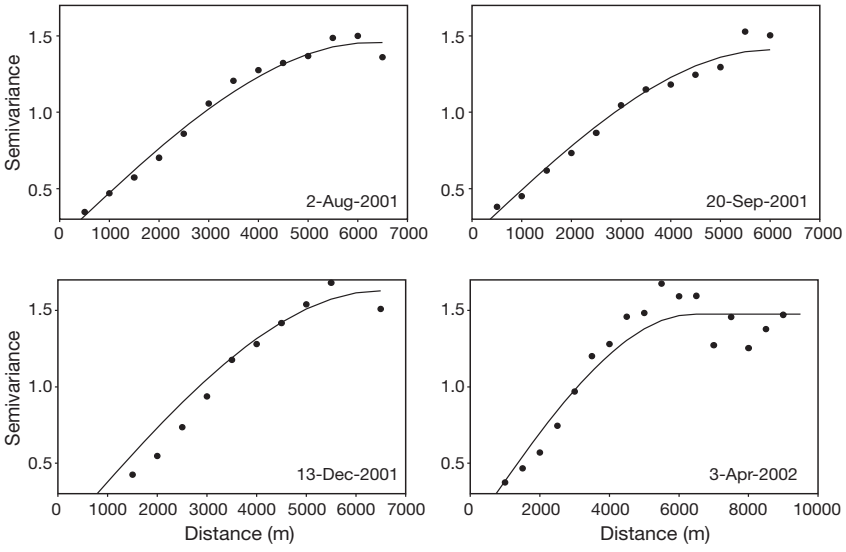

Fig. 4. Examples of semivariogram models for mapping surface temperature

sentation of the true distribution, we interpolated the data using ordinary kriging. This method was applied by Montávez et al. (2000) to map the UHIs of Granada (Spain). In contrast to other interpolation techniques, kriging assures optimal predictions according to the spatial variation in the data (Borrough & McDonnell 1998). In addition, the estimated values coincide with the values observed at measurement points. Moreover, kriging provides an estimate of the uncertainty of interpolation.

The predictions obtained using kriging methods are based on a weighted average of the data available in the *n* neighboring sampling point. The weighting is chosen so that the calculation is not biased and variance is minimal. Initially, a function that relates the spatial variance of the climatic variable must be determined using a semi-variogram model that adjusts the semi-variances between the climatic values at distinct spatial distances. Fig. 4 shows an example of several semi-variogram models of standardized thermal values on various days. In general, the semi-variances were adjusted by means of spherical semi-variogram models.

3.1.2. Continuous mapping of thermal data

The standardized thermal values were integrated in a GIS. The spatial distribution of temperature within the city is continuous, but the data obtained from car-transects are not. Therefore, to obtain a closer repre-

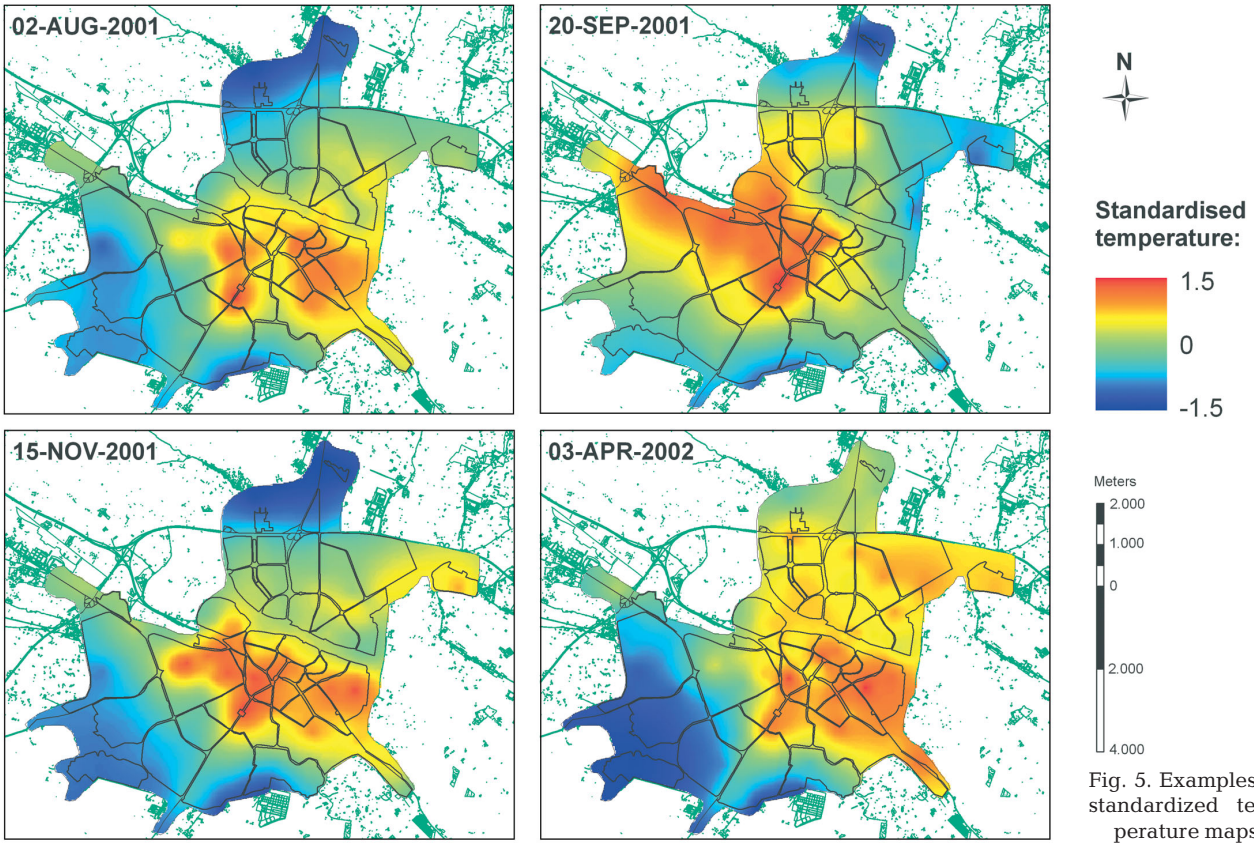

Fig. 5. Examples of standardized temperature maps

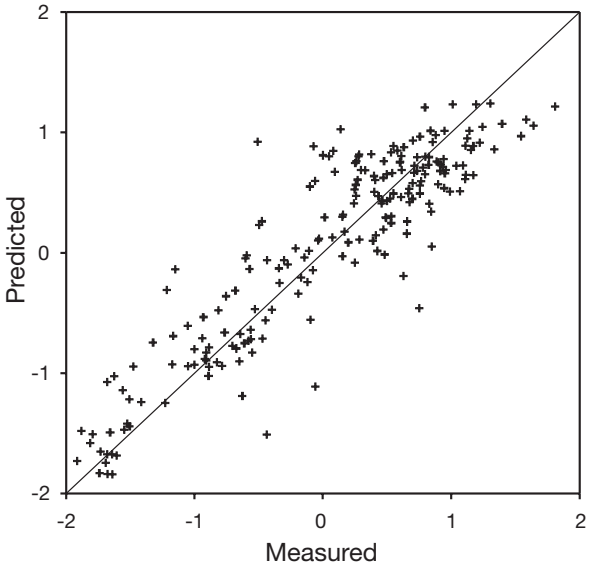

Fig. 6. Difference between measured temperature data and predicted data using bootstrap analysis and kriging estimation (data measured on 02/28/2002)

The maps were created using a grid cell size of 30 m. Fig. 5 shows various UHI patterns. In these maps, each 30×30 m grid cell (total: 53 000) contains standardized temperatures. Subsequent analyses were based on this spatial database, which was integrated in a GIS and composed by continuous maps instead of sampling points.

We used a cross-validation technique in a bootstrap routine to validate the results of the interpolation. Each sample point was removed and its value in the grid position was estimated by interpolation. The process is iterative and ends when all points have been removed from interpolation and their standardized temperature is estimated by means of the other points using kriging. Using the predicted values from cross-validation technique and the measured values, we calculated several error statistics for each map: root mean square error (RMSE), coefficient of determination (r^2) and agreement index (d) (Willmott 1982). Coefficients of determination between predicted and measured values oscillated between 0.85 and 0.9; RMSE was between 0.15 and 0.2, and the agreement index (d) was >0.95 in all cases. These results indicate the general agreement of estimates obtained by kriging. An example of measured versus predicted values is shown in Fig. 6. The solid line indicates a perfect coincidence of the estimates.

3.1.3. Estimation of UHI spatial patterns

We obtained the UHI distribution from a continuous spatial database of 27 grids. For this purpose, we used Principal Component Analysis (PCA), which allows common features to be identified and specific local characteristics to be determined (Richman 1986, Jollife 1990). PCA reduces a large number of interrelated variables to a few principal components that capture much of the variance of the original data set (Hair et al. 1998). We used PCA in the temporal (T) mode (see Jollife 1990) to analyse the spatial variability of the UHI. In this mode the variables are the distinct time observations (each of the 27 temporal samples) and the cases are the different locations (53 000 grid cells). A correlation matrix was selected for the analysis, because it provides a more efficient representation of the variance in the data set (Barry & Carleton 2001).

The criterion of component selection was an eigenvalue >1 (Hair et al. 1998). Components were rotated to obtain invariable spatial patterns. The rotation simplifies the spatial patterns of the variable studied (Barnston & Livezey 1987) and redistributes the final explained variance. The rotation procedure allows a clearer separation of components that maintain their orthogonality (Hair et al. 1998) and concentrates the loading for each PC onto the most influential variables. We used the Varimax rotation (Kaiser 1958), which is the most widely applied option because it produces more stable and physically robust patterns (Richman 1986, White et al. 1991).

Using PCA, we obtained standardized values for each component extracted in each grid cell. The empirical orthogonal function (EOF) values represent the correlation between each spatial component and the individual maps and determine the similarity between sample maps and the main spatial patterns of UHIs represented by components. High EOF values indicate a high similarity, while low values (near 0) show a low relationship between the 2 maps. In summary, the evolution of EOF values indicates the temporal representativeness of each spatial component.

3.2. Classification of wind direction

We used daily data of surface wind direction from the Zaragoza weather station. The data is recorded hourly, and we used the information that corresponded to the centalr time of the transects on a given day. The surface wind direction is reported in degrees and we classified the 27 days into 2 dominant directions, according to valley geography and dominant wind flow directions. The flow direction values from 45° to 225° were classified to SE flow, whereas those between 225° and 45° were classified as NW flow.

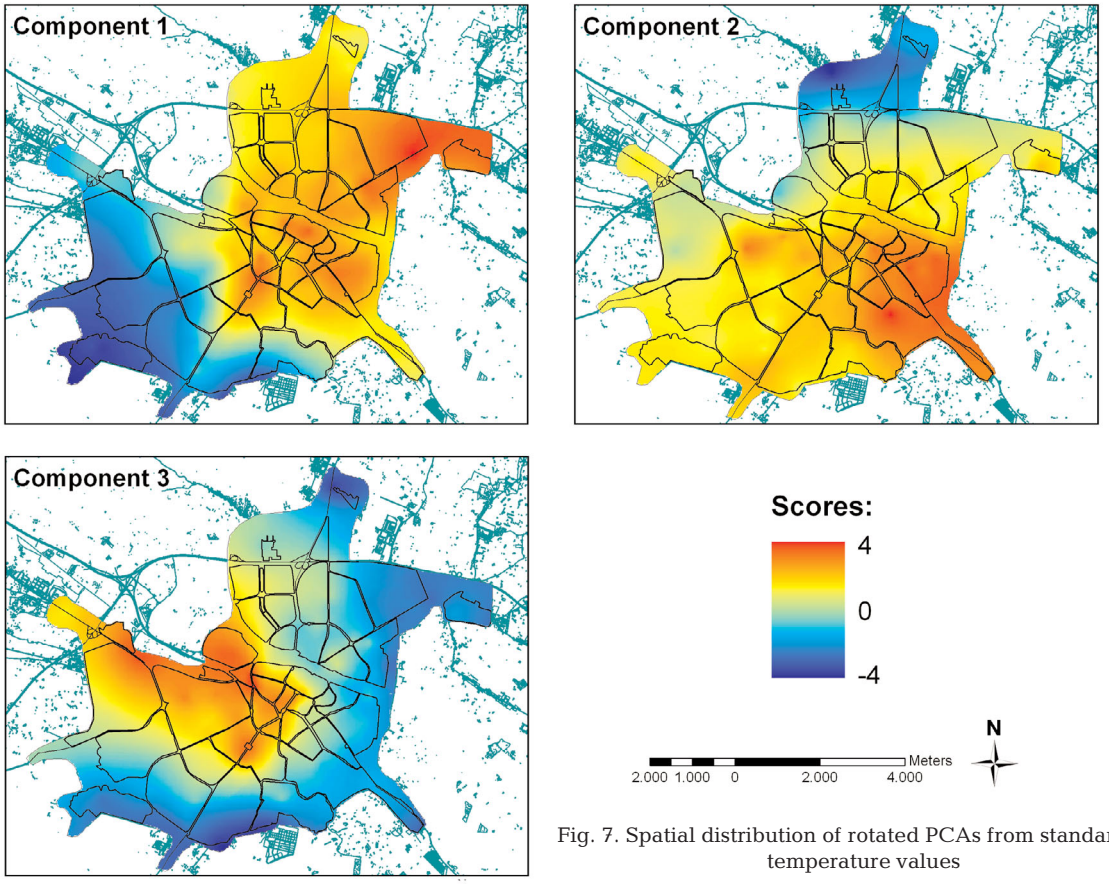

Fig. 7. Spatial distribution of rotated PCAs from standardized temperature values

3.3. Influence of wind direction on spatial patterns of the UHI

Relating the spatial patterns in temperature to surface wind direction is problematic, because temperature is measured on a spatial scale, while wind direction is assumed to be the same over the whole region. This problem was solved by extracting a small number of statistics from the spatial patterns obtained from PCA, and then a comparison of means (*t*-test) was performed to relate these summary statistics (EOFs) to the explanatory variable (surface wind direction); the Levene test was used to determine whether there were differences in the variances of the EOFs between the surface wind direction groups (Conover et al. 1981), because the variances of the 2 samples may be assumed to be equal or unequal (Snedecor & Cochran 1989). Significance of analysis was fixed at $p < 0.1$.

The EOF values indicate the similarity between general UHI patterns and the spatial configuration of UHI on the different days. For this reason, high EOF values corresponding to a wind direction will show a large effect of these atmospheric characteristics on UHI shape.

4. RESULTS

4.1. General spatial patterns of the UHI

The 3 first components explained 92.9% of the total variance (PC1: 40.5%; PC2: 37.2%; PC3: 15.1%). Other components obtained from the analysis did not explain a significant percentage of variance and were excluded.

We used GIS to map the standardized temperatures of PC1, PC2 and PC3 (Fig. 7). The spatial distribution of PC1 had a similar shape to that of the mean UHI mapped in Saz et al. (2003), with positive standardized values in the central and NE areas of the city (warm areas) and low values in the S and SW, on the high terraces of the Ebro River. PC2 indicated a displacement of the UHI to the SE, and PC3 showed a displacement to the NW. In PC2, cold areas were displaced to the N of the city while in PC3 the coldest areas were in the N, S and E.

EOF values obtained from the PCA (Fig. 8) indicated a high similarity between the spatial patterns shown in PC1 and PC2 and most of the daily thermal maps. Although a large percentage of days were well correlated with these 2 components, those most closely correlated with PC1 showed poor correlation with PC2

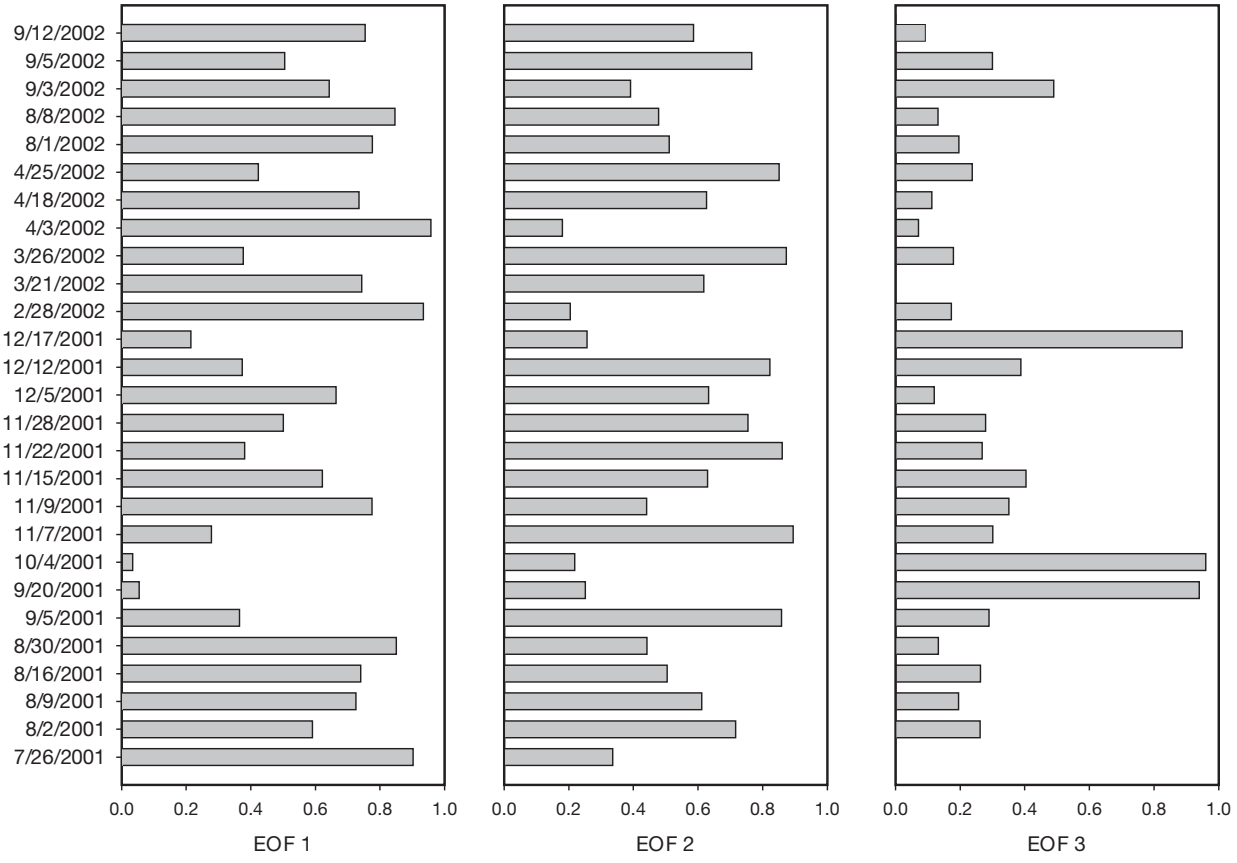

Fig. 8. Empirical orthogonal function (EOF) values corresponding to different days of measurement

and vice versa. Daily maps closely correlated with PC3 (12/17/2001; 10/4/2001; 9/20/2001) had poor correlation with PC1 and PC2.

These observations indicate that the shape of UHI in Zaragoza is not stable over time.

4.2. Influence of wind direction on UHI variability

Table 1 shows the results of the tests of effect of wind direction on the UHI (by means of the EOF values). For EOF1, the equality of variances cannot be assumed, as the variance of EOFs is higher for SE than for NW flows. The *t*-test (equal variance not assumed; Table 1) did not indicate statistically significant differences in EOF values between the 2 groups ($p < 0.1$). Therefore, PC1 does not show a statistically significant difference in UHI pattern as a function of NW or SE winds. Nevertheless, EOF1 values were more frequently related to NW winds (Fig. 9A). In addition, the analysis also indicated that the spatial patterns shown by Components 2 and 3 were related to wind direction. The *t*-tests indicated

Table 1. Results of the Levene's test for equality of variances and *t*-test for comparison of means (independent samples). Independent variables: EOF values; factor: surface wind direction (SE and NW)

		Levene's test		*t*-test		
		F	p	*t*	df	p (2-tailed)
EOF 1	Equal variances assumed	6.90	0.01	−1.90	25	0.069
	Equal variances not assumed			−1.48	8.65	0.174
EOF 2	Equal variances assumed	2.21	0.15	−2.46	25	0.021
	Equal variances not assumed			−2.07	9.68	0.066
EOF 3	Equal variances assumed	26.65	0.00	3.02	25	0.006
	Equal variances not assumed			2.04	7.42	0.079

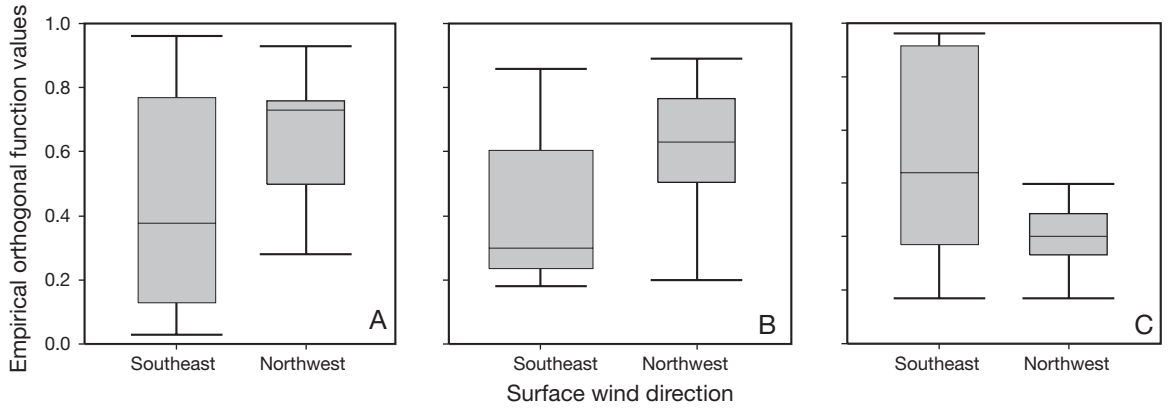

Fig. 9. EOF values for (A) PC1, (B) PC2 and (C) PC3 as a function of surface wind direction. Number of data points is 8 for SE winds, and 19 for NW winds

that equal variances may be assumed between the days with NW and SE flows for EOF2. Therefore, significant differences in the EOF values were influenced by wind direction. Unequal variances were assumed for EOF3, but significant differences were also found ($p < 0.1$).

EOF2 indicates that the spatial configuration of PC2 was more frequent on days with NW surface winds (high EOF values) (Fig. 9B). EOF3 indicated that the spatial configuration of PC3 was related to days with SE winds (Fig. 9C).

On days with NW winds, the UHI of Zaragoza has a similar shape to the spatial configuration of PC2 (displacement to the SE), and on days with SE surface winds the UHI is similar to the configuration of PC3. Nevertheless, the high variability in EOF3 values for days with SE winds shows a higher uncertainty regarding the shape of the UHI than on days with NW winds.

5. CONCLUSIONS

Spatial patterns of the UHI in Zaragoza (Spain) are not stable over time, and we identified 3 main types. PC1 showed the most frequent position of warm and cold areas, consistent with Cuadrat et al. (1993) and Saz et al. (2003). We also found a significant relationship between days with northwesterly surface winds (W,WNW, NW and NNW; 52% of the days) and a displacement of the UHI to the SE, and between SE winds (21% of the days) and displacement of the UHI to the west. Effects of surface wind direction on UHI shape or position have also been found by Gedzelman et al. (2003) and Szegedi & Kircsi (2003). UHI displacement affects bioclimatic comfort (Yan & Oliver 1996) and energy consumption in the city, as well as the dispersion of contaminants in the lower atmosphere (Junk et al. 2003). Therefore, analysis of the spatial and temporal behavior of UHIs may help city planners to improve urban management and contaminant control.

Acknowledgements. We acknowledge financial support from the following projects: BSO2002-02743, REN2003-07453, CGL2005-0408/BOS (funded by the Ministerio de Ciencia y Tecnología of Spain, and by FEDER); 'Programa de grupos de investigación consolidados', grupo Clima, Cambio Global y Sistemas Naturales, BOA 48 of 20-04-2005 (funded by the Government of Aragon); and 'Clima y calidad ambiental en la ciudad de Zaragoza' (funded by the Zaragoza City Council). Research of S.M.V.-S. was supported by a postdoctoral fellowship of the Ministerio de Educación, Cultura y Deporte of Spain).

LITERATURE CITED

Adebayo YR (1987) A note on the effect of urbanization on temperature in Ibadan. J Climatol 7:185–192

Arnfield AJ (2003) Two decades of urban climate research: a review of turbulence, exchanges of energy and water, and the urban heat island. Int J Climatol 23:1–26

Atkinson BW (1985) The urban atmosphere. Cambridge University Press, Cambridge.

Barnston AG, Livezey RE (1987) Classification, seasonality, and persistence of low-frequency atmospheric circulation patterns. Mon Weather Rev 115:1083–1126

Barry RG, Carleton AM (2001) Synoptic and dynamic climatology. Routledge, London

Beral-Guyonnet I (1997) Analyse spatiale des températures mensuelles dans l'agglomération lyonnaise. Rev Geogr Lyon 72:263–266

Borrough PA, McDonnell RA (1998) Principles of Geographical Information Systems. Oxford University Press, Oxford

Conover WJ, Johnson ME, Johnson MM (1981) A comparative study of tests for homogeneity of variances, with applications to outer continental shelf bidding data. Technometrics 23:351–361

Cuadrat JM (1993) Los climas urbanos en el Valle del Ebro. In: López-Gómez A (ed) El clima de las ciudades españolas. Cátedra, Madrid

Cuadrat JM, De la Riva J, López F, Martí A (1993) El medio ambiente urbano en Zaragoza. Observaciones sobre la isla de calor. Anal Univ Complutense (Madrid) 13:127–138

De la Riva J, Cuadrat JM, López F, Martí A (1997) Aplicación de las imágenes Landsat TM al estudio de la isla de calor térmica de Zaragoza. Geographicalia 35:24–36

Dimoudi A, Nikolopoulou M (2003) Vegetation in the urban environment: microclimatic analysis and benefits. Energy Build 35:69–76

Eliasson I (1994) Urban-suburban-rural air temperature differences related to street geometry. Phys Geogr 15:1–22
Gedzelman SD, Austin S, Cermak R, Stefano N, Partridge S, Quesenberry S, Robinson DA (2003) Mesoscale aspects of the Urban Heat Island around New York City. Theor Appl Climatol 75:29–42
Hair JF, Anderson RE, Tatham RL, Black W (1998) Multivariate data analysis. Prentice Hall, NY
Hogan AW, Ferrick MG (1988) Observations in nonurban heat islands. J Appl Meteorol 37:232–236
Jollife IT (1990) Principal component analysis: a beginner's guide. Part I: Introduction and application. Weather 45: 375–382
Junk J, Helbig A, Lüers J (2003) Urban climate and air quality in Trier, Germany. Int J Biometeorol 47:230–238
Kaiser HE (1958) The varimax criterion for analytic rotation in factor analysis. Psikometrica 23:187–200
Kidder SQ, Essenwanger OM (1995) The effect of clouds and wind on the difference in nocturnal cooling rates between urban and rural areas. J Appl Meteorol 34:2440–2448
Kuttler W, Barlag AB, Robmann F (1996) Study of the thermal structure of a town in a narrow valley. Atmos Environ 30: 365–378
Landsberg HE (1981) The urban climate. Academic Press, New York
Magee N, Curtis J, Wendler G (1999) The urban heat island effect at Fairbanks, Alaska. Theor Appl Climatol 64:39–47
Montávez JP, Rodríguez A, Jiménez JI (2000) A study of the urban heat island of Granada. Int J Climatol 20:899–911
Moreno MC (1994) Intensity and form of the urban heat island in Barcelona. Int J Climatol 14:705–710
Morris CJ, Simmonds I (2000) Association between varying magnitudes of the urban heat island and the synoptic climatology in Melbourne, Australia. Int J Climatol 20: 1931–1954
Morris CJ, Simmonds I, Plummer N (2001) Quantification of the influences of wind and cloud on the nocturnal urban heat island of a large city. J Appl Meteorol 40:169–182
Oke TR (1983) Bibliography of urban climate 1977–1980. WMO WCP-45, World Meteorological Organization, Geneva
Oke TR (1990) Bibliography of urban climate 1981–1988. WCAP-15, WMO/TD-No. 397, World Meteorological Organization, Geneva
Oke TR (1995) The heat island of the urban boundary layer: characteristics, causes and effects. In: Cermak JE (ed) Wind Climate in Cities. Kluwer, Norwell
Oke TR, Maxwell GB (1975) Urban heat island dynamics in Montréal and Vancouver. Atmos Environ 9:191–200
Philandras CM, Metaxas DA, Nastos PT (1999) Climate variability and urbanization in Athens. Theor Appl Climatol 63:65–72
Richman MB (1986) Rotation of Principal Components. J Climatol 6:29–35
Saaroni H, Ben-Dor E, Bitan A, Potcher O (2000) Spatial distribution and microscale characteristics of the urban heat island in Tel-Aviv, Israel. Landscape Urban Plan 48:1–18
Saz MA, Vicente-Serrano S, Cuadrat JM (2003) Spatial patterns estimation of urban heat island of Zaragoza (Spain) using GIS. In: Klysik K, Oke TR, Fortuniak K, Grimmond CSB, Wibig J (eds) Proc 5th Int Conf Urban Climate. World Meteorological Organization, Geneva, and University of Lòdz, Lòdz
Snedecor GW, Cochran WG (1989) Statistical methods, 8th edn. Iowa State University Press, Iowa City, IO
Szegedi S, Kircsi A (2003) The development of the urban heat island under various weather conditions in Debrecen, Hungary. In: Klysik K, Oke TR, Fortuniak K, Grimmond CSB, Wibig J (eds) Proc 5th Int Conf Urban Climate. World Meteorological Organization, Geneva, and University of Lòdz, Lòdz
Tereschenko IE, Filonov AE (2001) Air temperature fluctuations in Guadalajara, Mexico, from 1926 to 1994 in relation to urban growth. Int J Climatol 21:483–494
Unger J, Sumeghy Z, Zoboky J (2001) Temperature cross-section features in an urban area. Atmos Res 58:117–127
White D, Richman H, Yarnal B (1991) Climate regionalization and rotation of principal components. Int J Climatol 11:1–25
Willmott CJ (1982) Some comments on the evaluation of model performance. Bull Am Meteorol Soc 63:1309–1313
Winkler JA, Skaggs RH, Baker DG (1981) Effects of temperature adjustments on the Minneapolis-St Paul urban heat island. J Appl Meteorol 20:1295–1300
Yamashita S, Sekine K, Shoda M, Yamashita K, Hara Y (1986) On relationships between heat island and sky view factor in the cities of Tama River Basin, Japan. Atmos Environ 20:681–686
Yan YY, Oliver JE (1996) The CLO: a utilitarian unit to measure weather/climate comfort. Int J Climatol 16:1045–1056

Editorial responsibility: Nils Christian Stenseth, Oslo, Norway

Submitted: August 2, 2005; Accepted: October 25, 2005
Proofs received from author(s): November 18, 2005